# Reconstruction of a regional drought index in southern Sweden since AD 1750

Igor Drobyshev,[1,4] Mats Niklasson,[1] Hans W. Linderholm,[2]
Kristina Seftigen,[2] Thomas Hickler[3] and Olafur Eggertsson[5]

## Abstract

We used a network of eight pedunculate oak (*Quercus robur* L.) sites ($n_{trees}$ = 70) and one Scots pine (*Pinus sylvestris* L.) site ($n_{trees}$ = 53) to develop drought-sensitive master chronologies for the two areas in southern Scandinavia: a SW-area centred on 57°N 12.7°E and a NE-area centred on 58.8°N 18.2°E. The ratio of actual to equilibrium evapotranspiration (AET/EET) was used as a measure of drought during the growing season defined as the period with average daily temperatures above 9°C. Instrumental data were used to parameterize the relationship between tree-ring data and the drought index (DI) over 1922–2000 for the SW area and over 1922–1995 for the NE area. The DI reconstructions explained 29.7% (SW area) and 43.7% (NE area) of the variance in the observed DI index in the calibration period, and were extended back to AD 1770 for the SW area and to AD 1750 for the NE area. Reconstructed drought dynamics suggested strong decadal- and century-scale temporal variability and limited regional synchronicity over 1770–2000. Large variations in DI were observed in both regions in the second half of the 1700s. Dry conditions were synchronously reconstructed in both sub-regions during 1781–1784, 1853–1855, and, to a lesser degree, during 1974–1978. Over the 1945–1975 period the SW area exhibited a trend towards drier growing seasons, whereas no such trend could be identified for the NE area. Analysis of correlation maps indicated that regional DI dynamics reflected two different climate regimes, associated with the Kattegat area (SW reconstruction) and southeastern Swedish coast of the Baltic sea (NE reconstruction).

## Introduction

The dynamic nature of environmental conditions affecting ecosystems' functioning has being receiving increasing attention, primarily because of uncertainty concerning future climate variability (Hanssen-Bauer et al., 2005; Prentice et al., 1991; Rowell, 2005; Rowell and Jones, 2006). Recent studies reveal the complex temporal and spatial nature of natural processes and the important role of large-scale circulation processes which control climate dynamics (Brazdil et al., 2005; Bronnimann et al., 2007). Although temperature and precipitation regimes are intrinsically related to each other, independent reconstruction of these weather components are required to provide a sound basis for understanding historical dynamics of physiologically relevant growth parameters. Until recently, most attention in the literature has been given to the past and future dynamics of the temperature regime of the Northern Hemisphere (Briffa et al., 2004; Mann et al., 1999; Riedwyl et al., 2008; van Oldenborgh et al., 2009). In Europe, temperature reconstructions are currently available for Fennoscandia (Briffa et al., 1988; Grudd et al., 2002; Tuovinen et al., 2009), the Swiss Alps (Meier et al., 2007), and central and western Europe (Riedwyl et al., 2008; Xoplaki et al., 2005). Since the beginning of the twenty-first century considerable progress has also been made in reconstruction of past precipitation dynamics. Continuous and spatially explicit reconstructions were developed for different parts of the European subcontinent (Casty et al., 2005; Gimmi et al., 2007; Masson-Delmotte et al., 2005; Matti et al., 2009) and currently seasonal gridded precipitation reconstructions exist from AD 500 (Casty et al., 2007; Pauling et al., 2006). Despite advances in understanding millennium-scale variation in

drought conditions in Europe (Brazdil et al., 2005; Luterbacher et al., 2002), more research is needed on regional scales. For example, there is a need to increase the number of high-resolution precipitation proxies from Northern Europe, since the highest reconstructive skill of the available European reconstructions is found over the central and southern parts of the continent where most proxies are located (Pauling et al., 2006).

Reconstructing past variations in water availability can be useful when identifying dominant modes of atmospheric circulation related to physiological processes of tree growth. Despite its northern location, southern Sweden is affected by summer droughts, which results in regional negative growth anomalies. A study of recent oak growth trends revealed that such growth anomalies affect the growth in the following years and can be important drivers of biomass accumulation in forest ecosystems at above-annual timescales (Drobyshev et al., 2008). Future

[1]Swedish University of Agricultural Sciences, Sweden
[2]University of Gothenburg, Sweden
[3]Lund University, Sweden
[4]Université du Québec en Abitibi-Témiscamingue, Canada
[5]Iceland Forest Research Station Mogilsa, Iceland

**Corresponding author:**
Igor Drobyshev, Swedish University of Agricultural Sciences, Southern Swedish Forest Research Centre, P.O. Box 49, SLU, Alnarp, 230 53 Sweden
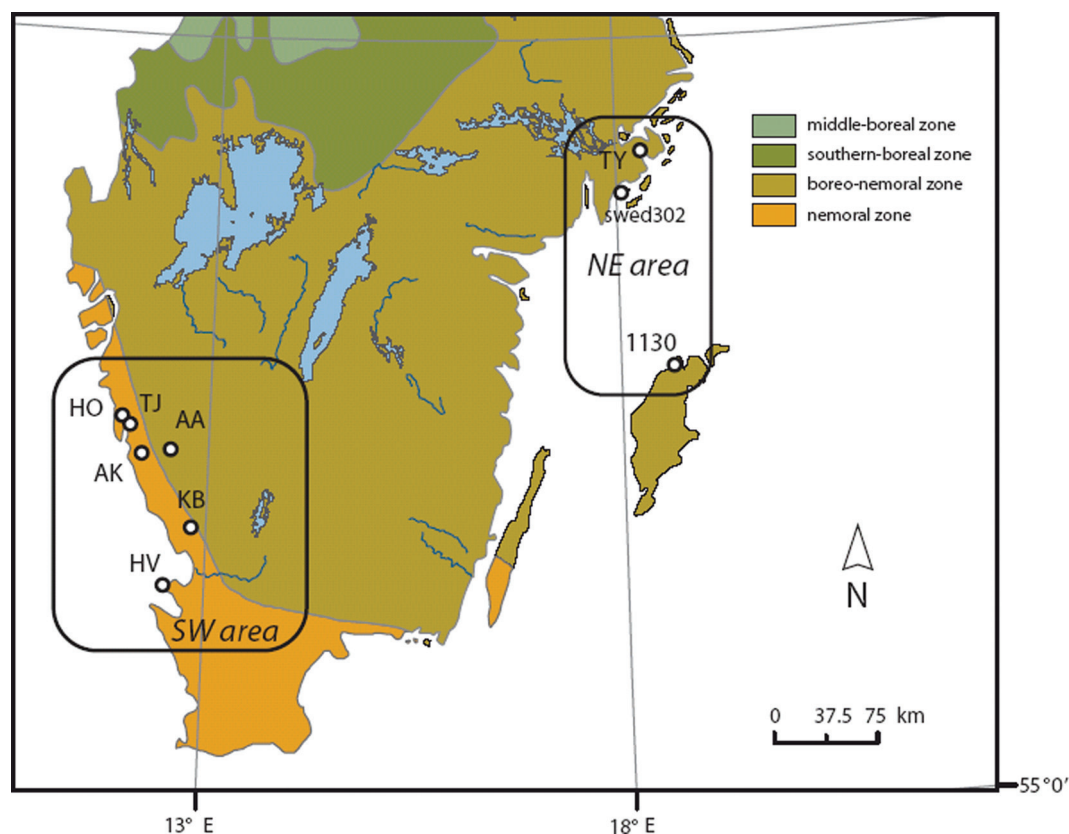Email: Igor.Drobyshev@slu.se

**Figure 1.** Study area and locations of sampling sites. With the exception of *swed302* site (Scots pine chronology), all sites were represented by pedunculate oak chronologies

climate projections suggest an increased frequency of drought episodes in parts of Northern Europe (Brabson et al., 2005; Rummukainen et al., 2001), which may imply even stronger dependence of tree growth on water availability in this region. It is thus of immediate practical interest to analyse the historical dynamic of water availability and to identify its likely driving factors.

In this study we present dendrochronological reconstructions of drought conditions for two areas in southern Sweden, centred on 57.0°N 12.7°E and 58.8°N 18.2°E, respectively. Although both areas are located in the temperate zone, there is considerable variation in the precipitation and temperature regimes between them. The southwestern part of the area receives one of the largest amounts of Atlantic-originated precipitation within southern Scandinavia (around 1000–1200 mm annually), with lower amounts of sunshine and temperature (Lundin, 2009; SMHI 2010). The northeastern part of the region is characterized by predominance of high-pressure systems during the growing period, which results in the high amount sunshine and moderate amount of precipitation (600–700 mm).

In contrast to traditional reconstruction of monthly or seasonal temperature/precipitation dynamics, in this study we employ a bioclimatic model to calculate a growing season drought index (DI). This index is believed to provide a realistic representation of the physiologically relevant dynamics of soil water availability during the growing season. The DI is the ratio of actual to equilibrium evapotranspiration (AET/EET) for the period when average daily temperatures reach above 9°C. AET is calculated as the minimum of the supply of water and the atmospheric demand in terms of EET, whereby the latter is driven by the amount of energy provided to the atmosphere through radiation (Jarvis and McNaughton, 1986). In turn, the water supply is proportional to

soil moisture (Federer, 1982), calculated for a one-layer bucket model (Prentice et al., 1993).

We use drought-sensitive oak (*Quercus robur* L.) and pine (*Pinus sylvestris* L.) chronologies to parameterize the relationship between tree-ring growth and DI. The selection of pedunculate oak as the main source of tree-ring data for this study is based on previously published results showing high sensitivity of oak growth to summer precipitation (Drobyshev et al., 2008; Kelly et al., 2002) and the presence of old oak trees on predominantly rocky substrates in both studied areas. Since no previously published DI reconstructions exist for Scandinavia, possibilities to compare our reconstruction with similar and independently derived time series are limited (although see Linderholm and Molin, 2005). We, therefore, use available precipitation reconstructions, as well as atmospheric circulation indexes, to discuss features of the developed DI series as well as probable drivers of regional soil water availability.

## Material and methods

### Study area

The oak trees were sampled in two areas of southern Sweden – in the region at the southwest Atlantic coast (NW corner of the area – 57.43°N 12.07°E; SE corner – 56.45°N 12.85°E; geographical centre – 57.01°N 12.64°E) and in the area close to the Baltic Sea coast including the island of Gotland (centre – 58.42°N 18.20°E; NW corner – 59.18°N 18.00°E; SE corner – 57.80°N 18.53°E) (Figure 1). Henceforth these two areas will be referred to as the SW-region and the NE-region, respectively. The mean annual temperature in this region ranges between 5°C and 8°C. The mean

**Table 1.** Statistical properties of chronologies used for the reconstructions. Values of Expressed Population Signal (EPS) are calculated for the detrended (ARSTAN) chronologies

| Variables | SW-area | NW-area | |
| --- | --- | --- | --- |
| | Oak chronology | Oak chronology | Pine chronology |
| Total chronology timespan | 1737–2003 | 1648–2002 | 1582–1995 |
| Period analysed | 1770–2000 | 1750–1995 | 1750–1955 |
| *n* | 45 | 25 | 53 |
| Mean series length | 107.5 | 191.3 | 130.4 |
| Mean no. trees per year | 18.2 | 16.0 | 21.7 |
| Mean sensitivity | 0.266 | 0.204 | 0.258 |
| Mean EPS[a] (min, max) | 0.939 (0.878, 0.998) | 0.917 (0.863, 0.940) | 0.929 (0.881, 0.957) |

[a]Calculated on the 40 year segments overlapped by 20 years.

temperature in January varies between −4°C and 0°C; and between 15°C and 16°C in July. There is a large precipitation gradient between the SW (up to 1200 mm/yr) and the NE (650 mm/yr) regions. The SW-area belongs to a climatic region with high growing season precipitation (>150 mm) while the NE area experiences droughts (< 50 mm) during the growing season (Lundin, 2009).

Prevailing winds in southern Sweden are typically westerly or southwesterly (Raab and Vedin, 1995). The growing season, typically defined as the period with average daily mean air temperature above 5°C, lasts for 180–240 days (Nilsson, 1996). Snow cover varies considerably within the study region and among years, and occurs from November–December to late February–March. The dominant soil type is till, where some areas are covered by a more rich clayed till from sedimentary limestone (Fredén, 2002). The sites used in the current study, however, were located on predominantly rocky and sandy substrates with limited water holding capacity.

The region stretches over both the nemoral and hemi-boreal phytogeographical zones (Ahti et al., 2004) and since a major part of the study region is a transition zone between the boreal and temperate biomes, both coniferous and deciduous trees are common. Norway spruce (*Picea abies* (L.) Karst.) and Scots pine (*Pinus sylvestris* L.) are the main coniferous species while oak (*Quercus robur* L. and *Q. petraea* (Matt.) Liebl.) and beech (*Fagus sylvatica* L.), together with small-leaved species (downy birch, *Betula pubescens* Ehrh. and aspen, *Populus tremula* L.), form the most prominent deciduous element of the vegetation.

### Site selection and chronology development

The study sites were selected to maximize the drought signal in ring-width dynamics and to provide the longest possible chronologies. A large network of oak chronologies (Drobyshev et al., 2008) was screened to identify sites and trees which complied with these criteria. Our selection strategy was to ensure that trees from selected sites covered both recent and more distant time periods. We therefore did not include in the analyses the sites with tree chronologies covering only nineteenth and twentieth centuries. This was done to avoid potential non-homogeneity of the proxy data, arising from variation in the number and spatial configuration of sites covering different time periods. Out of 51 sites and 668 trees screened, eight sites and 70 trees were selected for the analyses. During the selection process, individual tree chronologies were compared against a master chronology (average of the remaining chronologies) to identify series or parts of those with strong deviations from the common growth pattern. Similar

approach for initial tree selection has previously been used in Gouirand et al. (2008). From five sites (AK, TJ, AA, HO, HV, KB, Figure 1) 45 tree-ring series were used for the SW-area reconstruction (Figure 1, Table 1). For the NE-area reconstruction 25 series from two sites (TY and site # 0113, Figure 1) were used. Additionally, we used a Scots pine chronology swed302 developed by L.-Å. Larsson and available through ITRDB (http://hurricane.ncdc.noaa.gov/pls/paleo/fm_createpages.treering). This chronology contained 53 trees and revealed sensitivity to drought conditions in the preliminary analyses.

The sampling area within each site varied between 0.3 and 5 ha. At each site cores were taken along two radii from between 10 and 31 trees using an increment borer. On site KB several oak trees were sampled with a chainsaw and four chronologies were obtained from partial cross-sections. Core samples were taken at breast height, along two radii from each tree and after they were dried and mounted on wooden plates, they were polished using a belt sander, with up to a 400 grid band. The cores were measured using an LinTab measuring stage controlled by the software TSAP (Rinn, 1996). Two samples were cross-dated (Stokes and Smiley, 1968) and then averaged into single-tree chronologies. Dating was verified in CATRAS (Aniol, 1983) and COFECHA (Grissino-Mayer et al., 1997) computer programs.

### Statistical treatment of the chronologies

For each region, all selected oak chronologies were combined into a regional oak chronology. We used a conservative strategy during statistical treatment of the chronologies in the program ARSTAN_41d (Cook and Krusic, 2005). In an attempt to preserve low-frequency variance at decadal scales, we selected a combination of first negative exponential detrending and second linear detrending with any slope. Each tree-ring curve was modeled as an autoregressive process with the order selected by the first-minimum Akaike Information Criterion (AIC) (Akaike, 1974). The resulting chronology was produced by biweight averaging of single tree series under the condition of non-robust detrending option. Sample depth within a chronology varied between 7 and 29 trees for the SW-area oak chronology (1750–2000), between 7 and 22 trees for NE-area oak chronology (1770–2000) and between 15 and 31 trees for NE-area pine chronology (1750–1995). For the NE area, the resulting oak and pine chronologies were reduced down to one time series using principal component analysis. Chronology quality was assessed by the expressed population signal (EPS) statistics, which reflects the amount of common variance in single tree series,

preserved in the master chronology (Wigley et al., 1984). For each chronology, the EPS was calculated for 40-year segments, overlapping by 20 years.

## Calculation of the drought index (DI)

To calculate DI we re-programmed a version of the STASH model, which was originally developed to study the effect of climate changes on species distributions using factors considered to be physiologically important for the individual plant species (Sykes et al., 1996). The model was supplied with the values of monthly average temperature, total amount of monthly precipitation, and average cloudiness (% of open sky) and generated pseudo-daily values through a linear iteration process. Additional model parameters included soil-water holding capacity, timing of the growing season start, and latitude. The latter was used to determine solar angles and day lengths, both of which are needed for calculation of radiation balance.

In the model, DI was calculated as a ratio of actual to equilibrium evapotranspiration (AET/EET) over the period with average daily temperature above a defined threshold. The evaporative demand (EET) was understood as a function of net radiation and temperature, which approximated actual evapotranspiration when water supply is not limited. This measure is believed to be independent of humidity or surface resistances to transport of water vapour (Prentice et al., 1992). Such approximation suits situations well where EET is considered at above-stand (landscape and regional) scales (Jarvis and McNaughton, 1986). EET is, therefore, a measure of potential evapotranspiration (PET), driven by the amount of energy provided to the atmosphere through radiation (Jarvis and McNaughton, 1986). PET does not equal EET, since PET also depends on wind and the dynamics of the local boundary layer, which are generally difficult to model and are not considered during EET calculation.

Actual evapotranspiration (AET) is calculated with the same input variables (net radiation and temperature), but it is constrained by actually available soil water supply. The water supply is proportional to soil moisture (Federer, 1982), calculated for a one-layer bucket model (Prentice et al., 1993). AET is then considered as the lesser of instantaneous supply and demand. AET affects soil water balance, which is recalculated each day, based on the EET and precipitation. Additional details of model design and calculation algorithms are available in Prentice et al. (1992, 1993)

Similar to PDSI and PSI (Briffa et al., 1994), the DI is calculated in a cumulative fashion, integrating the interplay of water supply and demand at seasonal, annual, and intra-annual scales. However, unlike these indexes, DI takes into account radiation regime of a site over the whole year, which, together with temperature data, allows for a more biologically meaningful estimation of actual evapotranspiration demand. By using the DI in favor of PDSI, we also wanted to avoid known problems of using PDSI in situations where snow accumulation is a significant contributor to the soil water regime (Akinremi et al., 1996).

For the period 1922–2000, instrumentally measured DI, corresponding to an average AET/ETT, varied between 4.22 and 41.69 for the SW area and between 29.58 and 73.80 for the NE area. With relatively similar range of variability in this index (37.47 and 44.22 for SW and NE areas, respectively), the NE area is more prone to drought than the SW area. Values above 33.50 (for SW area) and 60.02 (for NE area) were within upper 5% percentile of the respective time series. For example, in the SW

area a strong drought event in 1992 corresponded to a DI value of 33.92 (above 97% percentile of respective distribution). In turn, years with abundant precipitation resulted in the low values of the drought index: 1999, 7.73, below 5% percentile of respective distribution, and 1985, 14.23, below 25% percentile.

In this study, the growth season was defined as the period with average daily temperatures above 9°C. The rationale for increasing the threshold from the commonly used value of 5°C was to focus on summer drought conditions and avoid the spring period when soil is generally wetter and evapotranspitation is minimal because of lack of a fully developed leaved crown. Setting such a threshold resulted in the start and the end of the growing season, on average, at the Julian dates 118 and 228 for SW area. The respective dates for NE area were 124 and 272.

The model utilized ALARM data, a data set of 0.16670° (approx. 16 km) gridded weather data (Mitchell and Jones, 2005). Data from three grid points were averaged for the SW-area (points 143–135, 144–137, and 138–142, according to ALARM data set notation) and from the two grid points – for the NE-area (points 177–151 and 178–143). Daily climatic data was produced from monthly values using linear interpolation method. The soil water holding capacity was set at 100 mm. Although the soil-water holding capacity is typically set to 150 mm in the previous studies (e.g. Sykes et al., 1996), we reduced the value to 100 mm since our sites were located on rocky substrates where limited water availability was likely. The DI was calculated for the period 1922–2000 for both areas.

## Calibration and testing of reconstruction accuracy

Multiple stepwise linear and non-linear regressions were used to evaluate the relationship between detrended chronologies and DI. Following the traditional calibration-verification approach we divided data into two parts representing early and late halves of the original data set. Relationships between reconstructed and the DIs modelled from the instrumental data were first calibrated on one part of the data set, and then verified on the part not used for calibration. The procedure was repeated with a different data set used for calibration/verification. Additionally, to calibrate the relationship between tree-ring chronology and DI we used the bootstrap approach (Efron and Tibshirani, 1994). We generated regression estimates on half of the original data set (40 years), which was resampled with replacement 500 times from the original data (79 years for SW or 73 years for NE area). This approach allowed us to use the whole period jointly covered by two data sets and to provide robust estimates of regression parameters, including their confidence limits. For the result presentation, reconstructed DI values were weighted against average DI over 1922–2000 in each of the subregions.

Reduction-of-error (RE), coefficient of efficiency (CE, Briffa et al., 1988) and the Sign tests (Fritts and Guiot, 1989) were used to evaluate the presence of predictive skill for each reconstruction. Values of RE and CE vary from $-\infty$ to $+1$ and positive values are indicative of reconstruction's predictive skill. The Sign test evaluates the number of agreements in the sign of departure from the respective means in both reconstructed and observed chronologies for each year. Significance of the Sign test indicates that direction of change in the chronology is more often correct than one could expect from random guessing.
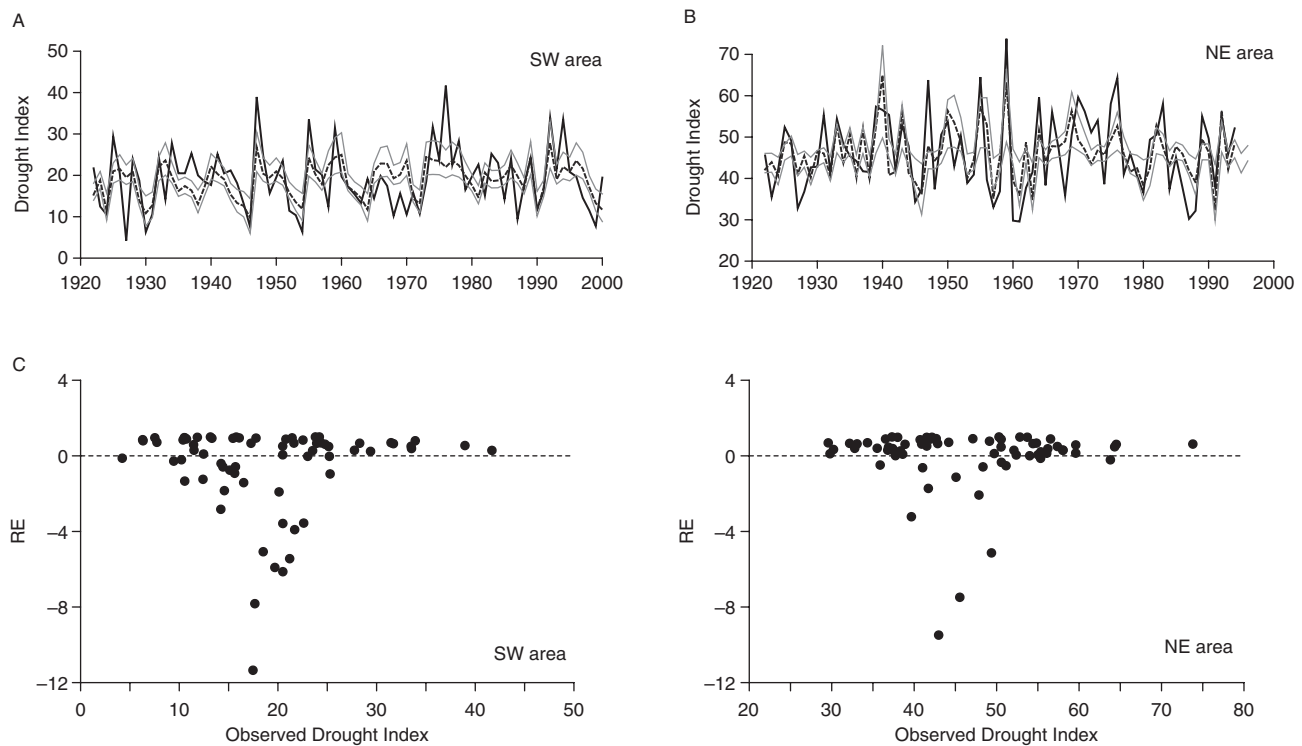
**Figure 2.** Chronologies of observed (black line) and reconstructed (dashed grey line) DI for the SW and NE areas (A and B, respectively) for the period 1922–2000. Thin grey lines are 95% confidence envelops of reconstructed DI. (C) Changes in reconstruction skill along a gradient in observed DI, expressed by the Reduction-of-error coefficient (RE)

DI reconstructions were compared against summer (JJA) precipitation reconstructions for two areas. Reconstructed precipitation series representing respective areas were obtained from Pauling et al. (2006) and Casty et al. (2007). Additionally, we used long instrumental precipitation record from two stations (SMHI 2010). For SW area we used total summer (JJA) precipitation data from the station at Lund (55°42′N 13°12′E, station code 5343, data available from 1748); for the NE area we used station at Stockholm (59°20′N 18°03′E, station code 9821, data available since 1786).

To assess similarity of reconstructions in respect to frequency domain, the spectral properties of the reconstructed indexes were obtained by wavelet analysis, which is recommended for time-frequency evaluation of non-stationary time series (Torrence and Compo, 1998). In our study, wavelet analysis employed a Morlet wavelet base (Torrence and Compo, 1998). This transformation is commonly used for characterizing variation in dominant frequencies of the time series in dendrochronological studies (e.g. Ogurtsov et al., 2008; Rigozo et al., 2005).

## Results

Master chronologies from the two areas showed similar and high levels of both among-tree correlations and EPS (Table 1). Over the considered time frames (1770–2002 for the SW area and 1750–1995 for the NE area) the chronologies quality exhibited little variability and showed tendencies towards increasing DI in the more recent time (Figure 2). With the exception of the earliest part of the pine chronology (1750–1790), the EPS values stayed well above the generally accepted level of EPS 0.85 (Wigley et al., 1984), indicating presence of consistent common signals in the chronologies. We found significant correlations between the NE and SE oak

chronologies over the 1770–2002 period ($r = 0.45$, $p < 0.001$, T-test = 7.5). For the NE area, the ARSTAN versions of the oak and pine chronologies entered PCA routine to produce a single variable, which subsequently was used in the reconstruction. PC1 explained 71.04% of variance (Eigen value −1.423).

Different linear equations were used to parameterize the relationship between tree-ring data and DI in the two areas. For the SW area, preliminary analyses, using step-wise multiple regression, indicated that the chronology value for the focal year (the year of the current growing season) was the only variable which entered linear regression with significant $b$ coefficient. For the NE area, coefficients for the current and the previous growing seasons were significant (Table 2) and, therefore, were included in the final equation.

Calibration and verification confirmed the significance of the regression coefficients and overall good predictive power of the parameterized linear equations for both regions (Table 2). Two alternative verification routines produced consistent results. First, analyses of non-overlapping calibration and verification demonstrated skill of tree-ring data to capture the DI dynamics (Reduction of Error, RE $\geq$ 0.182). For the verification equations, $R^2$ values ranged from 20.88 to 47.27%. For the SW area, early verification (1922–1961) with late calibration (1962–2000) was clearly superior over late verification and early calibration, $R^2$ being 36.50 and 20.88%, respectively. Second, the reconstruction skill was confirmed through Monte Carlo experiments on the complete periods (RE $\geq$ 0.299). The amount of DI variability explained by the chronologies during verification was 29.78 and 43.65% for SW and NE areas, respectively (Table 2, data on Monte Carlo experiment; Figure 2). The Monte Carlo experiment was also used to derive confidence limits for the reconstructed series (Figures 3 and 4).

**Table 2.** Verification of the drought index reconstructions

| Variables | SW-area | NE-area |
|---|---|---|
| *Calibration on the whole period* | | |
| $b_0$, t test, and *p* value | 36.01, $p < 10^{-18}$ | 46.09, $p < 10^{-59}$ |
| $b_1$, t test, and *p* value | −17.01, $p < 10^{-6}$ | −7.78, $p < 10^{-9}$ |
| $b_2$ | – | 2.64, $p = 0.014$ |
| $R^2$ adjusted | 29.00 | 42.71 |
| Overall regression *p* value | $< 10^{-6}$ | $< 10^{-9}$ |
| *Verification and reconstruction quality* | | |
| *1. Late verification (early calibration)* | | |
| Regression results | $R^2_{adj} = 20.88, p = 0.002$ | $R^2_{adj} = 47.27, p < 10^{-4}$ |
| T-value, *p* | 2.523 | 2.172, $p < 0.05$ |
| Sign test (no. agreements/total, *p*) | 23/39, $p > 0.05$ | 31/37, $p < 0.01$ |
| Reduction of Error, RE | 0.182 | 0.316 |
| Coefficient of efficiency, CE | 0.223 | 0.341 |
| *2. Early verification (late calibration)* | | |
| Regression results | $R^2_{adj} = 36.50, p < 10^{-4}$ | $R^2_{adj} = 39.46, p < 10^{-4}$ |
| T-value, *p* | 3.336 | 2.4624, $p < 0.01$ |
| Sign test (no. agreements/total, *p*) | 28/40, $p < 0.05$ | 29/38, $p < 0.01$ |
| Reduction of Error, RE | 0.348 | 0.473 |
| Coefficient of efficiency, CE | 0.393 | 0.111 |
| *3. Monte Carlo experiment (whole period calibration)* | | |
| Regression results | $R^2_{adj} = 29.78$ (10.23–50.50) $p = 0.009$ (0.083–$10^{-6}$) | $R^2_{adj} = 43.65$ (24.93–61.37) $p = 0.001$ (0.002–$10^{-7}$) |
| T-value, *p* | 4.413, $< 0.01$ | 3.1963, $< 0.01$ |
| Sign test (no. agreements/ total, *p*) | 50/79, 0.0316 | 59/74, $< 0.01$ |
| Reduction of Error, RE | 0.299 | 0.363 |
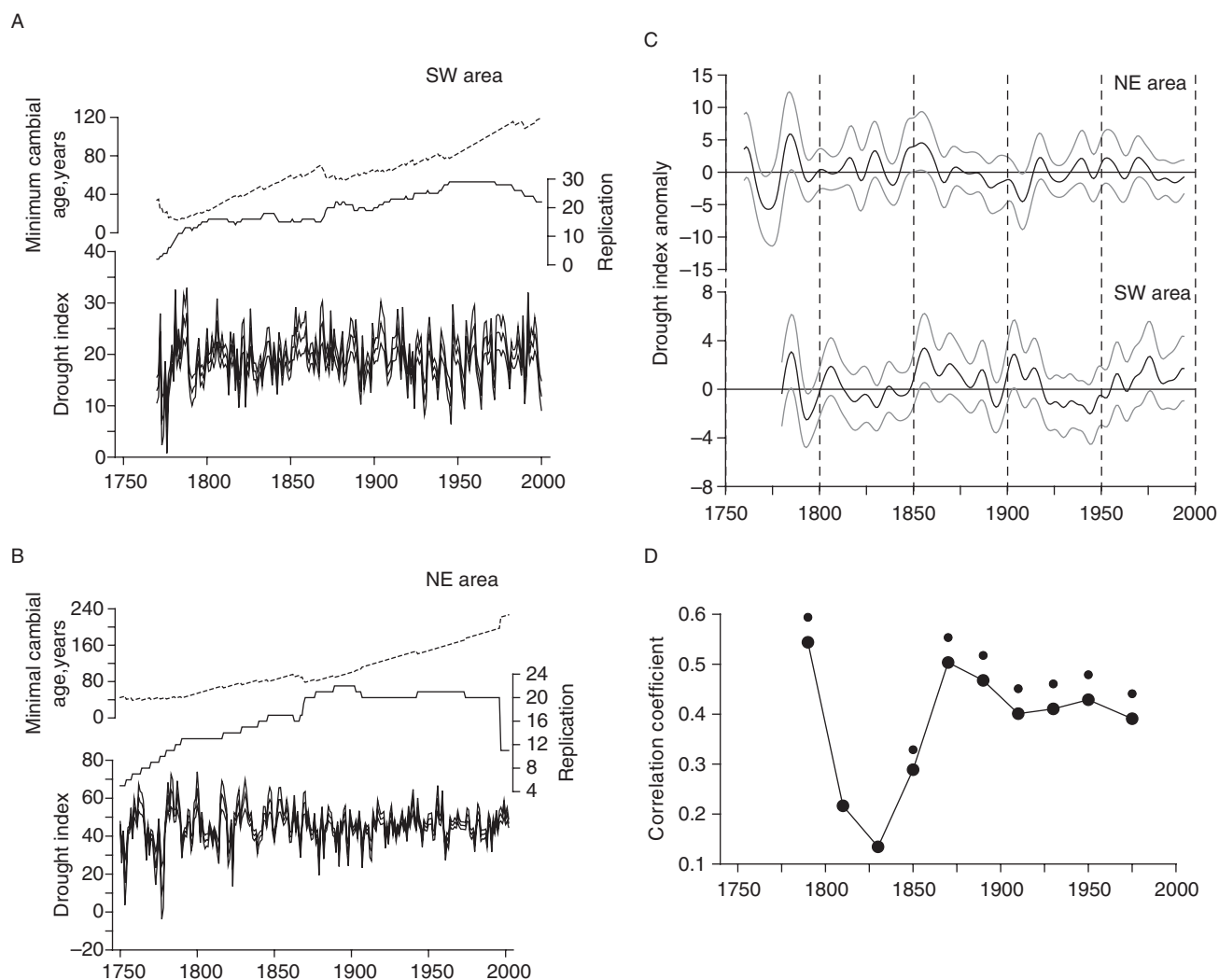


**Figure 3.** Full reconstructions of the growth season drought index for the SW (A) and NE (B) areas. Thick blank line is the reconstructed index with 95% confidence bands (thin black lines). Moving 5-year averages (thick grey line) are presented for each reconstruction and are redrawn together in (C) to facilitate visual comparison. Synchronicity between two master area curves, represented by Spearman correlation coefficient, is shown for the period 1770–1995 (D). Circles at respective dots indicate significance of correlation coefficient at 0.05
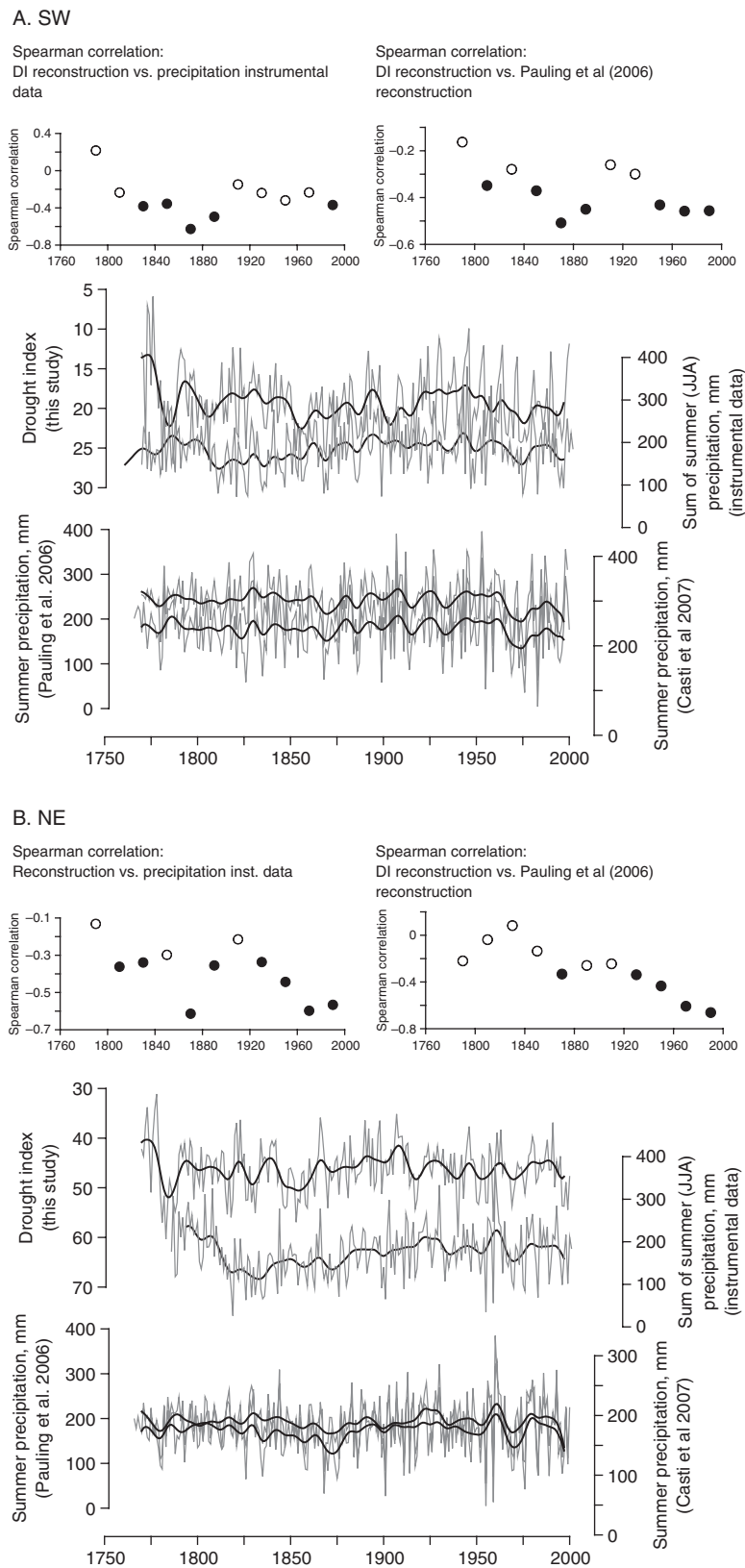
**Figure 4.** Comparison of DI reconstructions with instrumental precipitation data and previously published precipitation reconstructions. For each area DI chronology (the uppermost line) is presented together with total summer (JJA) precipitation from Lund (SW area) and Stockholm (NE area) as well as two precipitation reconstructions (Pauling et al., 2006 and Casti et al., 2007, two lowest lines). To facilitate visual comparison DI axis is inversed on both graphs. Values of Spearman correlation coefficient between DI and the instrumental data on total summer precipitation and preconstruction of Pauling et al. (2006) are graphed above of the respective graph (40 year time frame with 20 overlapping years). Filled circles indicate significance of correlation at $p < 0.05$

The amplitude of the extremes was under-represented in both reconstructions: for the SW reconstruction the observed range of values were 4.22–41.69 and the reconstructed 9.92–36.23. Similarly, for the NE reconstruction the ranges were 29.58–73.80 and 27.19–59.93 for actual and reconstructed values, respectively.
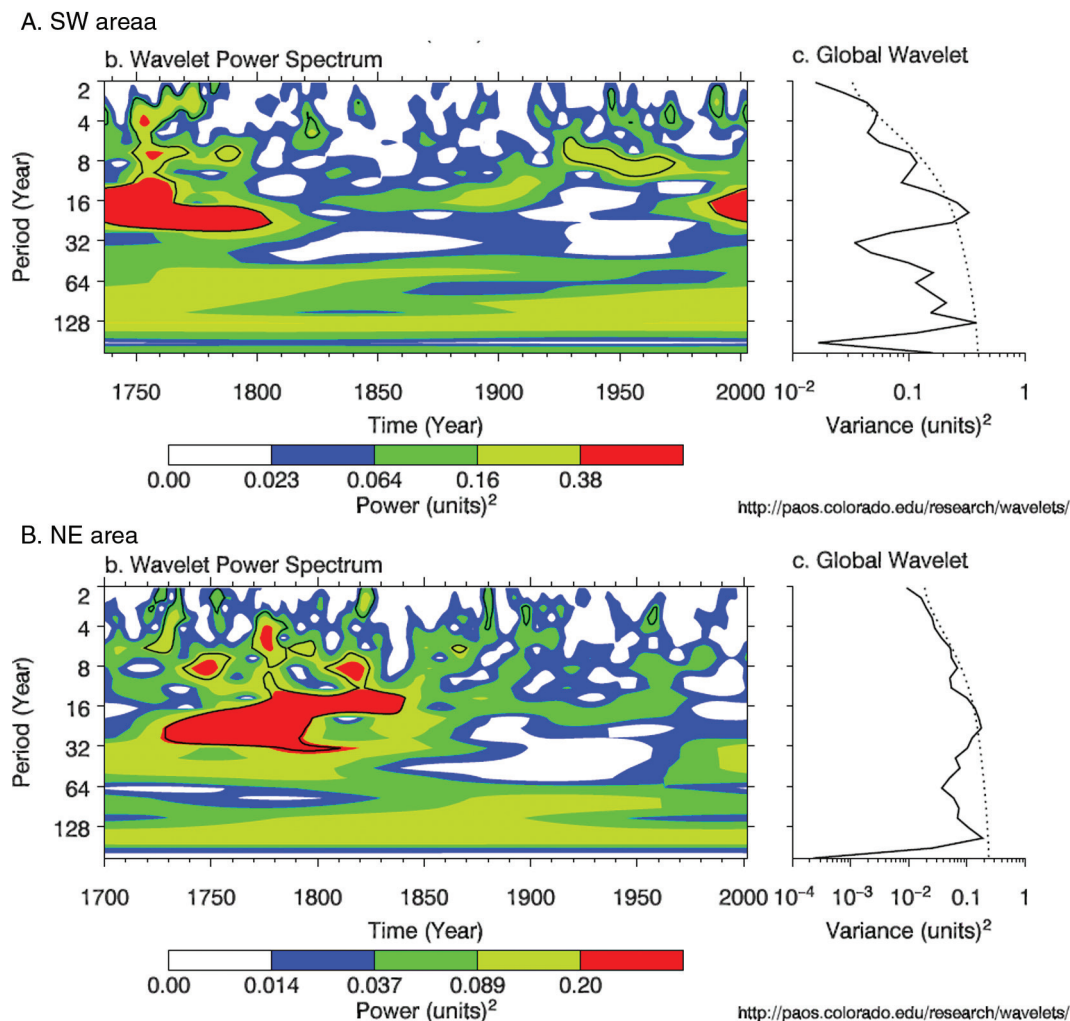
**Figure 5.** Wavelet analysis (Morlet wavelet transform) of reconstructed DIs. Significance in frequency variability is shown as a contour lines on the spectrum graphs and was estimated against red noise background spectrum (right side of each graph) at $p = 0.10$

The reconstructions suggested strong decadal- and century-scale temporal variability in DI dynamics but limited synchronicity of its annual variability between the two regions. Strong changes in the DI occurred in both regions in the second half of the 1700s. A period of drier growing season was centred around 1850, followed by a general trend towards wetter growing seasons in 1850–1900. In the SW area, a drier period was observed in the first decade of the twentieth century, while the NE area experienced wetter-than-average conditions during the same period. Over 1945–1975 the SW area exhibited a moderate trend towards drier growing seasons (Figure 3C). For the NE area, dynamics of DI over the twentieth century revealed a strong decadal variability but no long-term trend could be identified. Instead, a slight trend towards wetter growing seasons could be observed at the end of the twentieth century.

For the SW area, the correlation between instrumental data and the DI reconstruction stayed significant during most of the 1800s, while the correlation was non-significant for most of the 1900s period and second half of the 1700s (Figure 4). For the NE area, the correlations were typically significant since the early 1800s.

Annual synchronicity between the DI and precipitation reconstruction by Pauling et al.(2006), assessed by the Spearman correlation coefficient, tended to remain statistically significant after

1800 in the SW area and only after the beginning of the twentieth century in the NE area (Figure 4). Visual comparison of the decadal variability showed general agreements between DI dynamics and the precipitation reconstructions of Pauling et al. (2006) and Casty et al. (2007) over most of the nineteenth and twentieth centuries. However, the variability at above-decadal scales appeared to be more pronounced in our reconstructions: particularly for the SW area, the first halves of the 1800s and 1900s were generally less prone to drought, compared with the second halves of the respective centuries. This variability was not present in the precipitation reconstructions. Similarly, for the NW area, our reconstruction indicated the second half of the 1800s as a period with less drought-prone weather with no similar pattern being visible in the precipitation reconstructions.

Decadal-scale variability was the main mode of variability in the reconstructed DIs (Figure 5). Spectral analyses revealed a dominance of the 10–25 year frequencies in the earlier parts of both reconstructions. For the SW area, the effect was significant at $p = 0.10$ level during 1770–1800 and during the last decade of the twentieth century, and for the NE area during 1750–1840. For the SW area, a 40-year period centred around 1950 was characterized by significant manifestation of frequencies in the 7–10 year band. For the NE area, the period after 1840 did not reveal any statistically significant expression of particular frequency bands.
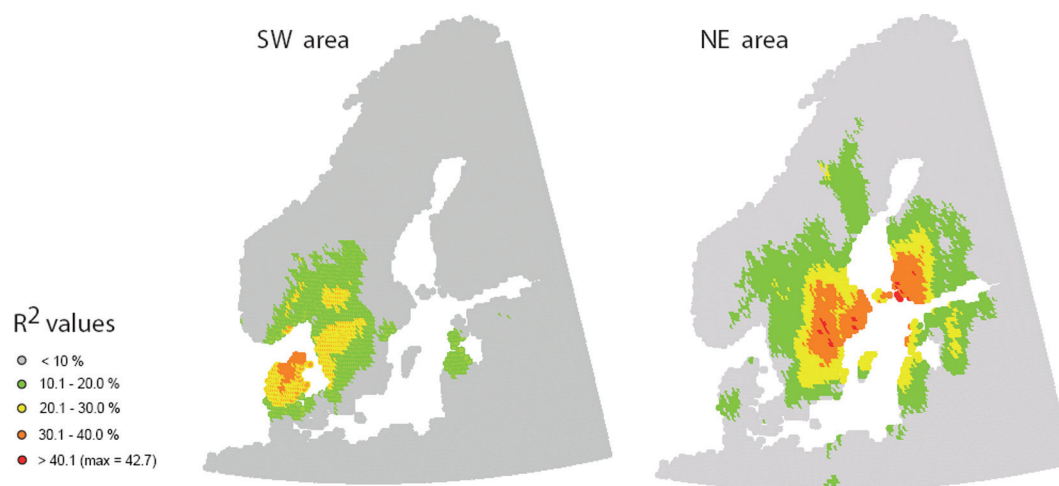
**Figure 6.** Point correlation maps between reconstructed DI and the DI modeled on the instrumental data for two studied areas. Correlation strength is represented by the amount of variation explained in linear regression ($R^2$). The data for the SW area is for 1922–2000 period, and for the NE area for 1922–1995 period

Analysis of correlation maps indicated regional differences in the DI dynamics. The SW and NE reconstructions reflected two different climate regimes associated with the Kattegat area (SW reconstruction) and southeastern Swedish coast of the Baltic sea (NE reconstruction) (Figure 6). The analysis indicated predictive power of both reconstructions outside the sampled area (Figure 6). Surprisingly, the highest predictive power of the SW reconstruction ($R^2$ above 30%) was observed over the territory of central and northern Denmark, limited by 56.0 and 57.4°N. A zone with moderate predictive power ($R^2 = 20$–30%) stretched over the central part of Denmark in the southwest direction from sampled area (down to 55.6°N), and up to 59°N in the northeast direction. Another zone was centred around 60°N 13°E. For the NE area, the highest prediction power of the reconstruction (> 40% $R^2$) was observed at several locations within 58.5°N 14°E and 59.5°N 18.0°E in Sweden, and in the most southwestern part of Finland (60.0°N, 22.0°E).

## Discussion

### *Reconstruction of drought indexes in southern Scandinavia*

Reconstructing historical dynamics of physiologically relevant environmental factors can advance our understanding of the actual effects of the climate change on forest ecosystems. In this study we calibrated a set of oak and pine chronologies against growing season DIs obtained from a physiological model, which, in turn, considered soil water balance as a product of water input and evaporative demand at a point scale. High values of the verification statistics obtained for both reconstructions support the use of oak and pine chronologies as proxies for past soil water regime in this part of Scandinavia. Despite the fact that oak typically has a deeply located root system and can have assess to soil water at deeper layers than most other tree species commonly found in the region (Rosengren and Stjernquist, 2004), it is sensitive to growing season precipitation even on sites that are not extremely dry (Drobyshev et al., 2008). Both oak and pine trees growing in shallow soil conditions likely experience even higher evapotranspiration demand and can therefore provide a proxy for past droughts.

Over the calibration period (1922–2000) the reconstructions captured both annual and decadal variability of the DI modelled on the instrumental data. However, the amplitude of the extremes in the observed drought indexes was better represented in the NE reconstruction than in the SW reconstruction (Figure 2). Limited representation of the actual variability in the instrumental records is a common problem of tree-ring derived reconstructions, arising from the linear calibration of drought indexes against tree-ring data and, most importantly, the biological nature of the chronologies. In oak, for example, buffering of the unfavourable environmental conditions occurs through the system of stomatal (Dickson and Tomlinson, 1996) and non-stomatal controls of carbon fixation (Epron and Dreyer, 1996). This naturally decreases variability in growth response as compared with the variability in the instrumental records. Nevertheless, considering the reconstruction quality across the whole DI gradient, the analyses suggested that both positive and negative extremes were both satisfactorily reproduced by the reconstructions, whereas the middle part of the gradient had the poorest reconstruction skill (Figure 2C).

High values of the DI were synchronously observed in both regions during 1781–1784, 1853–1855, and, to a lesser degree, during 1974(75)–1978(77) (Figure 3). This synchronicity suggests a dominance of high-pressure weather patterns in southern Sweden during these periods. In line with this suggestion, these periods coincide with periods of negative NAO index values, inferred from tree-ring data from sites above 60°N (Timm et al., 2004), as well as high pressure levels reconstructed from instrumental data (Bärring and Fortuniak, 2009).

We could not identify periods with low DIs synchronously observed across the whole of southern Sweden. This indicates that regional differences in precipitation are more important during periods of generally abundant soil moisture. For the SW area, three periods of below average DI values were found in 1789–1793, 1828–1833, 1882–1883, and 1943–1946. Temporal associations of these periods with anomalies in other weather indices are not evident. For example, only the most pronounced wet period around 1943–1946 coincided with a period of locally increased, as compared with the neighbouring decades, NAO index (Luterbacher et al., 2001) and an instrumental storminess index for southern Sweden (PC1 for Lund station, Bärring and Fortuniak, 2009: figure 7), which explains better water availability by increased westerly

transfer. It is worth noting that this period immediately followed an anomalous state of the troposphere and stratosphere of the Northern Hemisphere occurring between 1940 and 1942, and associated with a long-lasting El Niño event (Bronnimann et al., 2004). However, other supposedly wet periods in the SW region did not reveal any clear associations with available indices. For the NE area, the wettest periods were reconstructed for 1776–1779 and 1907–1910, with another generally wet period since 1978. These periods coincided with positive NAO indices and intensified storminess over the NE area (Bärring and Fortuniak, 2009; Luterbacher et al., 2001).

The lack of significant correlations between the DI reconstructions during first half of the 1800s (Figure 3D) may be indicative of asynchronous behaviour in the dynamics of soil water availability between SW and NE regions at that time. A 15-year period centred around 1828 was a pronounced wet period in the SW area during the 1800s. A similar, but much shorter event was visible in the DI reconstruction for the NE area. However, studies based on Scots pine chronologies and farmer's diaries from the east central Sweden (Linderholm and Molin, 2005; Linderholm et al., 2004) pointed out these years as a strong drought-prone period. Temperature reconstruction for northern Scandinavia suggests above-average temperatures in 1826–1831 (Briffa et al., 1988). Our results, therefore, indicate that this drought event did not affect the southwestern part of Sweden. Such lack of synchronicity is indirectly confirmed by comparison of reconstructed storminess indexes (Bärring and Fortuniak, 2009) indicating large variation in storminess between regions during that period.

## Comparison of DI with instrumental data and existing reconstructions

Comparison of our DI reconstruction with instrumental records and/or reconstructions of single variables used for calculation of the drought index is inherently ambiguous. Differences may arise as a result of variation in quality of one or both compared series, as well as because of actual differences in the dynamics of two variables. We nevertheless present such comparison with the purpose of highlighting features of newly produced reconstructions and identifying the periods which may require additional analysis and data acquisition.

Comparison of DI reconstructions with instrumental series indicated a generally variable degree of association between two variables and lack of a clear temporal pattern, suggesting the importance of cloud cover as a component of DI calculation. Association was better for the NE area than for the SW area (Figure 4), probably as a result of a more central location of the climate station in Stockholm in respect to the geographical locations of sampled sites and generally more continental climate in that subregion. The DI and precipitation reconstructions showed a higher degree of correlation towards the end of the twentieth century, suggesting that precipitation was closely connected to drought index dynamics since ~1950 (SW area) and ~ 1930 (NE area). Such a trend might indicate that a lack of correlation in the earlier periods could be a series quality issue. In both drought reconstructions lack of significant correlation with respective precipitation reconstructions was observed in the late nineteenth–early twentieth centuries (Figure 4). This period was characterized by a large change in the values of DI from high to lower values, an effect absent in precipitation series. An independent precipitation-sensitive pine chronology from the NE area (Linderholm et al., 2004) has shown

similarly large variation in growth increment in that period. Thus, such discrepancy in reconstruction results might be due to limited reconstruction skill of precipitation reconstructions at the turn of the twentieth century. Association of the DI and precipitation reconstructions disappears in the eighteenth and the first half of the nineteenth century, which might reflect the fact that precipitation reconstructions lacked proxies from the Northern Europe for the period prior to 1850 (Pauling et al., 2006).

Visual examination of the time series suggests that DI reconstructions, in general, show stronger low-frequency (~ 50-year range) variability than the one of both instrumental data and precipitation reconstructions (Figure 4). Besides a conservative approach employed during detrending of original tree-ring series, a nature of the DI index itself may cause preservation of this type of variability. In contrast to seasonal precipitation, DI is a cumulative measure of the current and previous years' soil water conditions, calculated in a continuous fashion across both dormant and growing seasons. DI calibration against original tree-ring series may therefore better reflect variability in soil water regime at above-annual timescales.

DI dynamics appear to be poorly synchronized with available temperature reconstructions. For example, high values of DI around 1770 in both DI reconstructions are indicative of an extremely drought-prone period in southern Fennoscandia, which is also visible in the published chronologies (Särö pine chronology, Linderholm et al., 2004: figure 6). However, in the northern Fennoscandian summer temperature reconstruction, this period (1777–1784) is identified as the one with below-average temperatures (Briffa et al., 1988). Further, only one prominent dry period recorded in the DI reconstructions, 1781–1784, coincided with a period of increased growth in the temperature-sensitive chronology developed for the Central Scandinavian Mountains (Linderholm, 2002). Such lack of synchronicity probably points to the difficulty in interpreting the temperature signal in terms of soil water dynamics. Although warmer summers in Scandinavia are indeed drier than colder summers (Casty et al., 2007: figure 3c), reconstruction of past drought should not be understood as the 'inverse' of precipitation reconstructions. In this study, the DI was calculated as a product of pseudo-daily temperature, precipitation, and cloud cover. The cloud cover variable is generally not considered in the context of dendrochronological reconstructions, though it can serve as an important modifier of tree response to environmental variation. A study of mean diurnal temperature range (DTR) and cloudiness at ten synoptic stations in the Nordic region did not reveal a stable relationship between temperature and cloudiness (Kaas and Frich, 1995), which suggests that the cloudiness may provide a unique contribution to the drought stress estimates.

## Spatial features of DI reconstruction

Our results point to regional differences in DI dynamics with SW and NE reconstructions reflecting two different climate regimes on the west and east coasts of southern Sweden. Higher $R^2$ of the SW reconstruction southwest of the sampled area indicated the importance of westerly winds, brining humidity to the region. The pattern of low $R^2$ values stretching in the northeast direction from the SW area is consistent with this explanation. The role of the North Atlantic jet stream in influencing temperature and precipitation regimes in southern Scandinavia is often connected to the intensity of North-Atlantic circulation pattern (Mares et al., 2002; Wanner et al., 2001). Enhanced anticyclonic activity, resulting from inversion of

the pressure patterns over the Atlantic Ocean (positive phase of the NAO), generally contributes to higher precipitation amounts and milder weather in this part of northern Europe (Bjorck et al., 2006; Luterbacher et al., 1999). The $R^2$ value fields indicated that the detectable influence of westerly transfer on growing season soil water regime may reach around 59°N. In turn, decay of $R^2$ values of SW reconstruction towards the eastern Swedish coast of the Baltic Sea suggested that local and strong anticyclonic activity prevents effective transfer of humid air into this part of the region. Generally, the spatial patter of $R^2$ values obtained for NE reconstruction implied importance of regional convection processes (Casty et al., 2007) in controlling soil water regime: a high-pressure system developing over central Scandinavia during the growing season covers a large part of southern Finland and southern Sweden within 58 and 61°N, as suggested by the $R^2$ value field.

The developed DI reconstructions are cumulatively representative of an area of the region within ~54.5°N 8.5°E and 62.0°N 24.4°E. Although the highest $R^2$ values stay below 45% for both reconstructions, we consider the reconstruction results generally satisfactory, taking into consideration the northerly location of the region, and difficulty in locating old and drought-sensitive trees. Since for both areas a large proportion of the grid points with high values of $R^2$ was located outside the areas sampled, expanding the sampled area for both subregions (towards central Denmark for SW area and towards southern Finland for NE area) should strengthen the drought signal and improve the reconstruction quality.

### Spectral frequencies of DI reconstructions

Our results suggest a different behaviour of drought index in the NE area in the period 1750–1850, as compared with the period after 1850. The earlier period was characterized by the dominance in the 15–25 yr frequency band, whereas DI variability during the more recent period was mostly restricted to below 15 yr frequencies. The period around 1750 marks the end of a century and a half long cold period in the Fennoscandian summer climate (Briffa et al., 1992; Gouirand et al., 2008; Grudd et al., 2002). Observed change in spectral properties of the temporal DI dynamics may, therefore, exemplify an association between drought conditions and changes in the large-scale circulation patterns. Analysis of the wavelet power spectrum of the annual and winter mean NAO indices showed a similar pattern with enhanced frequencies around the 32 year frequency band (Luterbacher et al., 1999; Wanner et al., 2001: figure 13). Freshwater and ice export into the North Atlantic (Delworth et al., 1997) and solar and/or oceanic influence (Meyers and Pagani, 2006) have been suggested as likely mechanisms behind this periodicity. Whatever may be the causes of these dynamics, an important observation in the context of the current study could be that soil water availability during the growing season and, therefore, the growth dynamics on water-stressed habitats reflects large-scale shifts in the NAO. It is also important to note that in this particular case, the association between the DI and NAO reconstructions involved the only the frequency domain and was not associated with particular state of the NAO. The first haft of the period in question (1750–1800) revealed a gradual evolution towards a state of positive NAO, culminating around the turn of the nineteenth century (Luterbacher et al., 2001) with maximum of westerly circulation mode also for the summer months (Jacobeit et al., 2003). The second half of the period (1800–1850) was instead characterized by a moderate decline in the NAO index.

Detection of frequency bands in a reconstructed chronology is dependent upon detrending procedures and length of single tree-ring chronologies used for building a master chronology (Briffa et al., 1996). Using a combination of negative exponential first detrending and second linear detrending treatments, we preserved variability at shorter frequencies ($< 10^2$), but might have affected frequency response at frequency ranges comparable with the mean length of the tree-ring series. In the current study, the series lengths were within 108–191 years (Table 1). Our reconstruction, therefore, cannot provide insight on long-term (~$10^2$ years) frequency ranges in DI variability.

### Conclusions and future projections

Calibrating tree-ring chronologies against bioclimatic variables is important for bridging climatic reconstructions with models of species response to environmental variation. This study shows the potential of this approach in respect to the historical dynamics of growing season drought conditions over southern Scandinavia. The developed DI reconstructions suggest strong decadal-scale variability and varying synchronicity of DI behaviour in southern Scandinavia. They also suggest that growing season drought may exhibit different long-term trends within a relatively small region. Although the most recent climate projections indicate that the warming during the twenty-first century is expected to increase with the distance from the coast and latitude (Hanssen-Bauer et al., 2005), behaviour of the DI for the NE area did not suggest a trend towards higher soil water deficit in the second half of the twentieth century (Figure 3). Instead, it is the DI of the SW region which showed a tendency to a moderate increase in the twentieth century (Figure 3C). As to the dynamics of the DI in the NE area, it showed no indication of long-term trend since ~ 1920 with somewhat less drought-prone conditions at the end of the twentieth century. Owing to the fact that most of the observed warming in the region is taking place during winter (Luterbacher et al., 2004), it may be only weakly correlated with growing-season soil water conditions. Since the latter is one of the crucial factors controlling growth and accumulation of biomass by vegetation, more focus on seasonal and subregional reconstructions and projections of future climate is warranted.

# References

Ahti T, Hämet-Ahti L and Jalas J (2004) Vegetation zones and their sections in northwestern Europe. *Annales Botanici Fennici* 5: 169–211.

Akaike H (1974) A new look at the statistical model identification. *IEEE Transactions on Automatic Control* 16: 716–723.

Akinremi OO, Mcginn SM and Barr AG (1996) Evaluation of the Palmer Drought index on the Canadian prairies. *Journal of Climate* 9: 897–905.

Aniol R (1983) Tree-ring analysis using CATRAS. *Dendrochronologia* 1: 45–53.

Bärring L and Fortuniak K (2009) Multi-indices analysis of southern Scandinavian storminess 1780–2005 and links to interdecadal variations in the NW Europe–North Sea region. *International Journal of Climatology* 29: 373–384.

Bjorck S, Rittenour T, Rosen P, Franca Z, Moller P, Snowball I et al. (2006) A Holocene lacustrine record in the central North Atlantic: Proxies for volcanic activity, short-term NAO mode variability, and long-term precipitation changes. *Quaternary Science Reviews* 25: 9–32.

Brabson BB, Lister DH, Jones PD and Palutikof JP (2005) Soil moisture and predicted spells of extreme temperatures in Britain. *Journal of Geophysical Research-Atmospheres* 110: 1–9.

Brazdil R, Pfister C, Wanner H, Von Storch H and Luterbacher J (2005) Historical climatology in Europe – The state of the art. *Climatic Change* 70: 363–430.

Briffa KR, Jones PD, Pilcher JR and Hughes MK (1988) Reconstructing summer temperatures in Northern Fennoscandinavia back to AD 1700 using tree-ring data from scots pine. *Arctic and Alpine Research* 20: 385–394.

Briffa KR, Jones PD, Bartholin TS, Eckstein D, Schweingruber FH, Karlen W et al. (1992) Fennoscandian summers from AD-500 – Temperature changes on short and long timescales. *Climate Dynamics* 7: 111–119.

Briffa KR, Jones PD and Hulme M (1994) Summer moisture variability across Europe, 1892–1991 – An analysis based on the Palmer Drought Severity Index. *International Journal of Climatology* 14: 475–506.

Briffa KR, Jones PD, Schweingruber F, Karlen W and Shiyatov S (1996) Tree-ring variables as proxy-climate indicators: Problems with low-frequency signals. In: Jones PD, Bradley S and Jouzel J (eds) *Climatic Variations and Forcing Mechanisms of the Last 2000 Years.* Berlin: Springer-Verlag, NATO ASI Series 141, 9–41.

Briffa KR, Osborn TJ and Schweingruber FH (2004) Large-scale temperature inferences from tree rings: A review. *Global and Planetary Change* 40: 11–26.

Bronnimann S, Luterbacher J, Staehelin J, Svendby TM, Hansen G and Svenoe T (2004) Extreme climate of the global troposphere and stratosphere in 1940–42 related to El Nino. *Nature* 431: 971–974.

Bronnimann S, Xoplaki E, Casty C, Pauling A and Luterbacher J (2007) ENSO influence on Europe during the last centuries. *Climate Dynamics* 28: 181–197.

Casty C, Wanner H, Luterbacher J, Esper J and Bohm R (2005) Temperature and precipitation variability in the european Alps since 1500. *International Journal of Climatology* 25: 1855–1880.

Casty C, Raible CC, Stocker TF, Wanner H and Luterbacher J (2007) A European pattern climatology 1766–2000. *Climate Dynamics* 29: 791–805.

Cook ER and Krusic PJ (2005) *Program ARSTAN. A Tree-ring Standardization Program Based on Detrending and Autoregressive Time Series Modeling, with Interactive Graphics*. Palisades NY: Tree-Ring Laboratory, Lamont Doherty Earth Observatory of Columbia University.

Delworth TL, Manabe S and Stouffer RJ (1997) Multidecadal climate variability in the Greenland Sea and surrounding regions: A coupled model simulation. *Geophysical Research Letters* 24: 257–260.

Dickson RE and Tomlinson PT (1996) Oak growth, development and carbon metabolism in response to water stress. *Annales des Sciences Forestieres* 53: 181–196.

Drobyshev I, Niklasson M, Linderson H and Sonesson K (2008) Influence of annual weather on growth of pedunculate oak in southern Sweden. *Annals of Forest Science* 65: DOI: 10.1051/forest:2008033.

Efron B and Tibshirani RJ (1994) *An Introduction to the Bootstrap*. Chapman & Hall.

Epron D and Dreyer E (1996) Starch and soluble carbohydrates in leaves of water-stressed oak saplings. *Annales des Sciences Forestieres* 53: 263–268.

Federer CA (1982) Transpirational supply and demand: Plant, soil, and atmospheric effects evaluated by simulation. *Water Resources Research* 18: 355–362.

Fredén CE (2002) *Geology. The National Atlas of Sweden*. Stockholm: SNA Förlag.

Fritts HC and Guiot J (1989) Methods of calibration, verification, and reconstruction. In: Cook ER and Kairiukstis LA (eds) *Methods of Dendrochronology. Application in the Environmental Sciences*. Kluwer, 163–217.

Gimmi U, Luterbacher J, Pfister C and Wanner H (2007) A method to reconstruct long precipitation series using systematic descriptive observations in weather diaries: The example of the precipitation series for Bern, Switzerland (1760–2003). *Theoretical and Applied Climatology* 87: 185–199.

Gouirand I, Linderholm HW, Moberg A and Wohlfarth B (2008) On the spatiotemporal characteristics of Fennoscandian tree-ring based summer temperature reconstructions. *Theoretical and Applied Climatology* 91: 1–25.

Grissino-Mayer HD, Holms RL and Fritts HC (1997) *International Tree-ring Data Bank Program Library Manual*. Tucson AZ: Laboratory of Tree-Ring Research, University of Arizona.

Grudd H, Briffa KR, Karlen W, Bartholin TS, Jones PD and Kromer B (2002) A 7400-year tree-ring chronology in northern Swedish Lapland: Natural climatic variability expressed on annual to millennial timescales. *The Holocene* 12: 657–665.

Hanssen-Bauer I, Achberger C, Benestad RE, Chen D and Forland EJ (2005) Statistical downscaling of climate scenarios over Scandinavia. *Climate Research* 29: 255–268.

Jacobeit J, Wanner H, Luterbacher J, Beck C, Philipp A and Sturm K (2003) Atmospheric circulation variability in the North-Atlantic–European area since the mid-seventeenth century. *Climate Dynamics* 20: 341–352.

Jarvis PG and McNaughton KG (1986) Stomatal control of transpiration: Scaling up from leaf to region. *Advances in Ecological Research* 15: 1–49.

Kaas E and Frich P (1995) Diurnal temperature-range and cloud cover in the Nordic countries – Observed trends and estimates for the future. *Atmospheric Research* 37: 211–228.

Kelly PM, Leuschner HH, Briffa KR and Harris IC (2002) The climatic interpretation of pan-European signature years in oak ring-width series. *The Holocene* 12: 689–694.

Linderholm HW (2002) Twentieth-century Scots pine growth variations in the central Scandinavian Mountains related to climate change. *Arctic Antarctic and Alpine Research* 34: 440–449.

Linderholm HW and Molin T (2005) Early nineteenth century drought in east central Sweden inferred from dendrochronological and historical archives. *Climate Research* 29: 63–72.

Linderholm HW, Niklasson M and Molin T (2004) Summer moisture variability in east central Sweden since the mid-eighteenth century recorded in tree rings. *Geografiska Annaler Series A-Physical Geography* 86A: 277–287.

Lundin L (2009) Humiditet under vegetationsperioden. http://www-markinfo.slu.se/sve/klimat/hum.html. Uppsala: Institutionen för skoglig marklära, SLU.

Luterbacher J, Schmutz C, Gyalistras D, Xoplaki E and Wanner H (1999) Reconstruction of monthly NAO and EU indices back to AD 1675. *Geophysical Research Letters* 26: 2745–2748.

Luterbacher J, Xoplaki E, Dietrich D, Jones PD, Davies TD, Portis D et al. (2001) Extending North Atlantic Oscillation reconstructions back to 1500. *Atmospheric Sciences Letters* 2: 114–124.

Luterbacher J, Xoplaki E, Dietrich D, Rickli R, Jacobeit J, Beck C et al. (2002) Reconstruction of sea level pressure fields over the Eastern North Atlantic and Europe back to 1500. *Climate Dynamics* 18: 545–561.

Luterbacher J, Dietrich D, Xoplaki E, Grosjean M and Wanner H (2004) European seasonal and annual temperature variability, trends, and extremes since 1500. *Science* 303: 1499–1503.

Mann ME, Bradley RS and Hughes MK (1999) Northern hemisphere temperatures during the past millennium: Inferences, uncertainties, and limitations. *Geophysical Research Letters* 26: 759–762.

Mares I, Mares C and Mihailescu M (2002) NAO impact on the summer moisture variability across Europe. *Physics and Chemistry of the Earth* 27: 1013–1017.

Masson-Delmotte V, Raffalli-Delerce G, Danis PA, Yiou P, Stievenard M, Guibal F et al. (2005) Changes in European precipitation seasonality and in drought frequencies revealed by a four-century-long tree-ring isotopic record from Brittany, western France. *Climate Dynamics* 24: 57–69.

Matti C, Pauling A, Kuttel M and Wanner H (2009) Winter precipitation trends for two selected European regions over the last 500 years and their possible dynamical background. *Theoretical and Applied Climatology* 95: 9–26.

Meier N, Rutishauser T, Pfister C, Wanner H and Luterbacher J (2007) Grape harvest dates as a proxy for Swiss April to August temperature reconstructions back to AD 1480. *Geophysical Research Letters* 34: 1–6.

Meyers SR and Pagani M (2006) Quasi-periodic climate tlelconnections between northern and southern Europe during the 17th–20th centuries. *Global Planetary Change* 54: 291–301.

Mitchell TD and Jones PD (2005) An improved method of constructing a database of monthly climate observations and associated high-resolution grids. *International Journal of Climatology* 25: 693–712.

Nilsson NE (1996) *Forests. Swedish National Atlas*. Stockholm: SNA Förlag.

Ogurtsov MG, Raspopov OM, Helama S, Oinonen M, Lindholm M, Jungner H et al. (2008) Climatic variability along a north-south transect of Finland over the last 500 years: Signature of solar influence or internal climate oscillations? *Geografiska Annaler Series A-Physical Geography* 90A: 141–150.

Pauling A, Luterbacher J, Casty C and Wanner H (2006) Five hundred years of gridded high-resolution precipitation reconstructions over Europe and the connection to large-scale circulation. *Climate Dynamics* 26: 387–405.

Prentice IC, Sykes MT and Cramer W (1991) The possible dynamic-response of northern forests to global warming. *Global Ecology and Biogeography Letters* 1: 129–135.

Prentice IC, Cramer W, Harrison SP, Leemans R, Monserud RA and Solomon AM (1992) A global biome model based on plant physiology and dominance, soil properties and climate. *Journal of Biogeography* 19: 117–134.

Prentice IC, Sykes MT and Cramer W (1993) A simulation model for the transient effects of climate change on forest landscapes. *Ecological Modelling* 65: 51–70.

Raab B and Vedin H (1995) *Klimat, sjöar och vattendrag. Sveriges National Atlas*. Stockholm: SNA Förlag.

Riedwyl N, Luterbacher J and Wanner H (2008) An ensemble of European summer and winter temperature reconstructions back to 1500. *Geophysical Research Letters* 35: 1–5.

Rigozo NR, Nordeman DJR, Echer E, Vieira LEA, Echer MPS and Prestes A (2005) Tree-ring width wavelet and spectral analysis of solar variability and climatic effects on a Chilean cypress during the last two and a half millennia. *Climate of the Past Discussions* 1: 121–135.

Rinn F (1996) *TSAP – Time Series Analysis and Precipitation, Version 3 Reference Manual*. Heidelberg.

Rosengren U and Stjernquist I (2004) *Gå på djupet! Om rotdjup och rotprodukiton i olika skogstyper. SUFOR report*. ISBN 91-576-6617-2. Lund: SUFOR Project.

Rowell DP (2005) A scenario of European climate change for the late twenty-first century: Seasonal means and interannual variability. *Climate Dynamics* 25: 837–849.

Rowell DP and Jones RG (2006) Causes and uncertainty of future summer drying over Europe. *Climate Dynamics* 27: 281–299.

Rummukainen M, Raisanen J, Bringfelt B, Ullerstig A, Omstedt A, Willen U et al. (2001) A regional climate model for northern Europe: Model description and results from the downscaling of two GCM control simulations. *Climate Dynamics* 17: 339–359.

SMHI (2010) Meteorologiska stationer. Månadssummor nederbörd och lufttemperatur. Available online at http://www.smhi.se

Stokes MA and Smiley TL (1968) *An Introduction to Tree-ring Dating*. Chicago IL: University of Chicago Press.

Sykes MT, Prentice IC and Cramer W (1996) A bioclimatic model for the potential distributions of north European tree species under present and future climates. *Journal of Biogeography* 23: 203–233.

Timm O, Ruprecht E and Kleppek S (2004) Scale-dependent reconstruction of the NAO index. *Journal of Climate* 17: 2157–2169.

Torrence C and Compo GP (1998) A practical guide to wavelet analysis. *Bulletin of the American Meteorological Society* 79: 61–78.

Tuovinen M, McCarroll D, Grudd H, Jalkanen R and Los S (2009) Spatial and temporal stability of the climatic signal in northern Fennoscandian pine tree-ring width and maximum density. *Boreas* 38: 1–12.

van Oldenborgh GJ, Drijfhout S, van Ulden A, Haarsma R, Sterl A, Severijns C et al. (2009) Western Europe is warming much faster than expected. *Climate of the Past* 5: 1–12.

Wanner H, Bronnimann S, Casty C, Gyalistras D, Luterbacher J, Schmutz C et al. (2001) North Atlantic Oscillation – Concepts and studies. *Surveys in Geophysics* 22: 321–382.

Wigley TML, Briffa KR and Jones PD (1984) On the average value of correlated time series, with applications in dendroclimatology and hydrometeorology. *Journal of Climate and Applied Meteorology* 23: 201–213.

Xoplaki E, Luterbacher J, Paeth H, Dietrich D, Steiner N, Grosjean M et al. (2005) European spring and autumn temperature variability and change of extremes over the last half millennium. *Geophysical Research Letters* 32: 1–4.